Transient spectral hole-burning studies of the R2 line in ruby

Riesen, Hans; Riesen, Nicolas; Schubert, Nathan; Szabo, Alexander

Publisher's version / Version de l'éditeur:
https://doi.org/10.1016/j.cplett.2009.04.074
Chemical Physics Letters, 475, 1-3, pp. 10-14, 2009

Dmn 4/09

Transient spectral hole-burning studies of the R_2 line in ruby.

Hans Riesen [a*], Nicolas Riesen[a] , Nathan Schubert[a] and Alex Szabo[b]

[a]*School of Physical, Environmental and Mathematical Sciences, The University of New South Wales, ADFA, Northcott Drive, Canberra, ACT 2600, Australia*
[b]*Institute for Microstructural Sciences, National Research Council of Canada 1200 Montreal Road, Ottawa, Ontario K1A 0R6, Canada*

*Author for correspondence: e-mail h.riesen@adfa.edu.au
Fax: ++61 (0)2 6268 8017

Abstract
We report transient spectral-hole-burning studies of the $R_2(\pm 1/2)$ line in 130 and 20 ppm ruby between 2.4 and 70 K. The homogeneous linewidth Γ_h, is found to be 142 ± 6 MHz at 2.4 K for both 20 and 130-ppm crystals; this value is in agreement with the T_1 value of 1.1 ns ($\Gamma_h = 1/2\pi T_1$=140 MHz) for the $2\bar{A}$ state obtained by Rives and Meltzer who used pulsed, non-selective laser excitation. The linewidth is dominated by a direct one-phonon relaxation process $2\bar{A} \rightarrow \bar{E}$ up to 50 K whereas at higher temperatures two-phonon Raman scattering becomes dominant. Cross-relaxation and spin-lattice relaxation times significantly affect pseudo-CW experiments.

1. Introduction

Ruby (Al_2O_3:Cr(III)) has served as an archetypal system for the development of optical and laser spectroscopy of impurity ions in insulators over the last 140 years. Luminescence based on the R-lines ($^4A_2 \leftarrow ^2E$) transitions was reported by Becquerel as early as the second half of the nineteenth century [1]. In the high impact paper by Tanabe and Sugano, ruby was employed as the model system in the development of a detailed ligand field theory in the 1950s [2]. In 1960 Maiman demonstrated the first laser action using a ruby rod at the Hughes Aircraft research laboratories [3]. Kurnitt, Abella and Hartman conducted the first photon echo experiment in ruby [4]. Then in the beginning of the 1970s Szabo reported the first luminescence line narrowing and the first transient spectral hole-burning experiment in the solid state [5,6] employing the R_1-line of ruby. Szabo *et al* continued to refine the hole-burning work on the R_1-line and a series of detailed investigations has been published over the last three decades [7-11]. In another major milestone McFarlane *et al* demonstrated photon-echoes in the superhyperfine limit [12]. In an early and highly influential paper on thermal broadening and shifts of electronic transitions of impurity centres in the solid state, McCumber and Sturge investigated and analysed the R-lines of ruby [13]. Their data analysis was limited to temperatures above 78 K since the inhomogeneous broadening is the dominant contribution to the linewidth at lower temperatures.

We have recently undertaken time-resolved transient hole-burning experiments on the R_1 line in ruby with chromium(III) concentrations of 20 and 0.6 ppm. In a 20 ppm crystal cross-relaxation is still a dominant effect, limiting the lifetime of the spectral hole. However, a 0.6 ppm ruby crystal, in a low magnetic field of a few mT parallel the crystal *c*-axis, exhibits hole lifetimes given by the spin lattice relaxation time [14].

Somewhat surprisingly, it appears that the R_2-line has not been investigated in detail by spectral hole-burning. The present paper reports transient spectral hole-burning results for 130 and 20 ppm rubies. At low temperatures the linewidth of the R_2 line is limited by a direct one phonon relaxation process from the upper to the lower ^{2}E level ($2\overline{A} \rightarrow \overline{E}$); in some early work the time T_1 for this process was indirectly (from spin-lattice relaxation experiments) determined to be 0.3 ns [15]. In contrast, Kurnitt *et al* determined a relaxation time of 2.75 ns for this process, a value that may have been affected by a phonon bottleneck that develops due to the high powers used in the photon echo experiment [16]. In more recent work, Rives and Meltzer determined the relaxation time to be T_1=1.1 ns by direct measurements, employing pulsed laser excitation [17]. The current paper investigates hole-burning properties of the R_2 line, providing an accurate way of determining T_1. The temperature dependence of the R_2 line is reinvestigated by hole-burning experiments up to 70 K. It is also shown that cross-relaxation significantly affects pseudo-continuous wave (CW) experiments.

2. Experiment

Ruby boules, grown by the Verneuil (flame fusion) process, were provided by Hrand Djevahirdjian SA, Monthey, Switzerland. The crystals were cut and polished parallel and perpendicular to the crystal *c*-axis with diamond-impregnated tools.

Spectral hole-burning experiments were conducted with a temperature and current stabilised diode laser (Hitachi HL 6938MG). The temperature and current were controlled by a Thorlabs TCLDM9 TEC mount in conjunction with a Thorlabs TEC2000 temperature controller and an ILX Lightwave ultralow-noise current source model LDX-3620.

The current of the laser was kept constant during the burn period and then rapidly scanned with a triangular ramp with a period of 400 μs. A Stanford Research Instruments synthesized function generator model DS345 was used for the current modulation.

In pseudo-continuous wave (CW) hole-burning experiments, the laser frequency was kept constant for ~1 ms and then scanned by a triangular ramp within 400 μs over 5-40 GHz at a repetition rate of 1 kHz.

Pulsed (8 ms pulse width; 1 Hz pulse repetition rate) experiments were conducted by passing the laser through a mechanical shutter (Vincent Uniblitz VS14S1T0) that was controlled by a Uniblitz VMM-T1 driver/timer. The laser frequency was kept constant during the initial phase of the pulse (1.2-6 ms) and then swept over ~5 GHz within 400 μs. In all experiments the laser was focussed onto the sample after attenuation by a polarizing film and a neutral density filter with OD=1. The effective power level at the sample was thus ca. 300 μW.

The samples were cooled by a Janis/Sumitomo SHI-4.5 closed-cycle refrigerator capable of reaching 2.5 K. The crystals were embedded with cry-con grease on the cold finger.

3. Results and Discussion

Polarized absorption and transient hole-burning spectra, obtained under pseudo-CW (steady state conditions), are illustrated in Figure 1. The inhomogeneous width of the $R_2(\pm 1/2)$ transition is about 9 GHz for the 130-ppm and 20-ppm samples and about 6 GHz for a 0.6 ppm sample. This is about 4-6 times wider than the width observed for the

R-lines in Czochralski grown crystals [8]. Figure 1a shows polarized absorption spectra for the R_2 line in a 20-ppm ruby. The effect of hole-burning into the $R_2(\pm 1/2)$ transition of a 0.6-ppm sample in σ polarization is illustrated in Figure 1b where a significant reduction of the absorbance A across the entire absorption profile is observed; indeed this reduction is larger than the depth of the resonant hole. In Figure 1c the unpolarized absorption spectrum, with and without hole-burning into the $R_2(\pm 1/2)$ transition, is shown for a 20-ppm sample. A pronounced drop in absorbance over the entire profile of the $R_2(\pm 1/2)$ line and an increase in absorbance across the inhomogeneous lineshape of the $R_2(\pm 3/2)$ transition is observed. The depth of the resonant hole and the sidehole is much less than the change of absorbance in the overall absorption profile. Finally, Figure 1d shows the unpolarized hole-burning difference spectrum, $\Delta A(\nu)$, for a very shallow hole in the $R_2(\pm 1/2)$ transition of a 130-ppm ruby sample. $\Delta A(\nu)=\log_{10}(I_{nb}(\nu)/I_b(\nu))$ where $I_{nb}(\nu)$ and $I_b(\nu)$ are the transmitted laser intensities without and with a burn period, respectively.

The transient hole-burning experiments are strongly affected by cross-relaxation between resonant and non-resonant ions in the $^4A_2$ ground state and this leads to a decrease and increase of the entire inhomogeneously broadened $R_2(\pm 1/2)$ and $R_2(\pm 3/2)$ lines, respectively, upon hole-burning into the $R_2(\pm 1/2)$ line. The cause for this behaviour is the effect of cross-relaxation together with the long spin-lattice relaxation time at 2.5 K [6,8,14]. Upon burning into the $R_2(\pm 1/2)$ line about two thirds of the excited ions are deactivated by $R_1(\pm 3/2)$ luminescence, ending in the $\pm 3/2$ spin level of the $^4A_2$ ground state; cross-relaxation between the resonant and non-resonant ions then occurs and thus the population of non-resonant ions in the $\pm 3/2$ Kramers doublet of the $^4A_2$ ground state increases significantly over the entire inhomogeneous distribution, depleting the $\pm 1/2$ spin state. Spin-lattice relaxation is too slow to counteract this build-up of non-thermalised $\pm 3/2$ population. The resonant hole in the $R_2(\pm 1/2)$ line and the associated side-hole at +11.3 GHz in the $R_2(\pm 3/2)$ line are obscured by this effect, and are only minor dips on top of significant changes in the overall absorption profile. The resonant hole (at zero offset) and the sidehole (at +11.3 GHz) of the resonant ions are indicated by arrows in Figures 1c and d. We have previously shown by hole-burning experiments in the R_1 line, that cross-relaxation even occurs in 0.6 ppm ruby but can be eliminated by the application of a (low) external magnetic field B||c in such dilute samples [14].

Figure 2 shows temperature effects in pseudo-CW experiments in comparison with pulsed measurements. It is obvious that the effective hole-depth in pseudo-CW experiments is strongly temperature dependent between 2.5 and 10 K. Again, this is due to the depletion of the overall absorbance; at 10 K spin-lattice relaxation is fast enough to counteract this effect. The pulsed experiments are not affected by cross-relaxation at the 1 Hz repetition rate since the system has enough time to thermalise.

Figures 3 and 4 illustrate spectral holes in the $R_2(\pm 1/2)$ line at 2.4 K as obtained by 1 Hz-pulsed experiments with burn periods ranging from 1.2 to 6.3 ms. The holewidth increases with increasing holedepth as is expected. This is illustrated In Figure 4b. We have conducted this experiment between 2.5 and 70 K and have obtained the homogenous linewidth as a function of temperature by extrapolation to zero holedepth for all temperatures. At 2.5 K we obtained a homogeneous linewidth of 142±6 MHz; this is a lifetime limited linewidth and provides directly a value for the $2\overline{A} \rightarrow \overline{E}$ relaxation time T_1 via the simple expression (1).

$$\Gamma_h = \frac{1}{2\pi T_1} \tag{1}$$

The linewidth corresponds to a value of T_1=1.12±0.04 ns which is in perfect agreement with the value of 1.1 ns obtained by Rives and Meltzer [17].
The temperature dependence of the homogeneous linewidth is summarised for the 20 and 130 ppm samples in Figure 5 where we also show the early data of McCumber and Sturge [13].
Hsu and Skinner have refined a nonperturbative approach for the broadening of the zero-phonon linewidth of impurities in crystals caused by quadratic electron-phonon coupling [18]. Approximating the density of acoustic phonon states by the Debye model, and using the expression for a direct one-phonon relaxation process following temperature dependence results for the R_2 linewidth

$$\Gamma = \Gamma_0\left(1+\frac{1}{\exp(\Delta/k_BT)-1}\right)$$
$$+\frac{\omega_D}{4\pi^2}\int_0^1 dx \ln\left[1+9\pi^2W^2x^6\frac{\exp(xT_D/T)}{(\exp(xT_D/T)-1)^2}\left(\left\{1+W(1+3x^2+\frac{3}{2}x^3\ln\left[\frac{1-x}{1+x}\right])\right\}^2+W^2\frac{9\pi^2}{4}x^6\right)^{-1}\right] \tag{2}$$

where W is the quadratic coupling constant, T_D is the Debye temperature, k_B is the Boltzmann constant, $\hbar\omega_D = k_BT$, and $\Gamma_0 = 1/2\pi T_1$ (T_1 is the lifetime of the $2\bar{A}$ level). In the weak coupling limit, |W|<<1, the second term reduces to the well-known T^7 expression given in the original paper by McCumber and Sturge [13], and the expression (2) simplifies to

$$\Gamma = \Gamma_0\left(1+\frac{1}{\exp(\Delta/k_BT)-1}\right)+\frac{9}{4}W\omega_D(T/T_D)^7\int_0^{T_D/T} dx\left[x^6\frac{\exp(x)}{(\exp(x)-1)^2}\right] \tag{3}$$

The data in Figure 5 is well described by using equation (2) with the parameters W=-0.277, T_D=935 K and Γ_0=142 MHz. A reasonable fit is also obtained by using W=+1.01. We note here that values of W=-0.282 or W=1.39 were reported in reference [18]. The Debye temperature T_D=935 K is the value obtained from heat capacity measurements [19]; in contrast, a significantly lower value T_D=760 K has to be applied when equation (3) is used to fit the data in Figure 5 [13].
The linewidth is dominated by the one-phonon relaxation process up to 50 K. Above this temperature two-phonon Raman scattering processes become dominant leading to a rapid increase of the width. The two contributions are individually plotted in Figure 5.

4. Conclusions

Spectral hole-burning work has generally been conducted on the lowest-excited state over the last 30 years and higher-lying excited states of transition metal ions and complexes were only the subject of a few investigations [20]. Higher-lying transitions are usually

subject to fast direct relaxation processes [21] and hence display rather broad hole-widths. Nevertheless, the present work illustrates that valuable information on higher-lying states can be obtained by hole-burning experiments. Transient spectral hole-burning experiments conducted in the present work provide an accurate determination of the $2\overline{A} \rightarrow \overline{E}$ relaxation time. The resulting value of T_1=1.12 ns at liquid helium temperatures is in perfect agreement with previous measurements by pulsed non-selective laser excitation.

Acknowledgement

We are grateful to Ms K. Djevahirdjian of Hrand Djevahirdjian SA, Monthey, Switzerland for providing us with the ruby boules of various concentrations. The Australian Research Council is acknowledged for financial support of our research program (ARC Discovery Project DP0772426).

References

[1] A.E. Becquerel, La Lumiere, ses causes et ses effets (Paris: Didot, 1867-1868) (reproduction: Microopaque. New York, N.Y.; Readex Microprint Corporation, 1968).
[2] S. Sugano, Y. Tanabe, J. Phys. Soc. Jap. 13 (1958) 880.
[3] T.H. Maiman, Nature 187 (1960) 493.
[4] N. A. Kurnitt, I. D. Abella, S. R. Hartmann, Phys. Rev. Lett. 15 (1964) 567-568.
[5] A. Szabo, Phys. Rev. Lett. 27 (1971) 323–326.
[6] A. Szabo, Phys. Rev. B 11 (1975) 4512.
[7] P.E. Jessop, T. Muramoto, A. Szabo, Phys. Rev. B 21 (1980) 926.
[8] P.E. Jessop, A. Szabo, in Laser Spectroscopy V, ed. A. McKellar, T. Oka, B.P. Stoicheff, Springer-Verlag (1981) p. 408.
[9] A. Szabo, T. Muramoto, R. Kaarli, Phys. Rev. B 42 (1990) 7769.
[10] A. Szabo, R. Kaarli, Phys. Rev. B. 44 (1991) 12307.
[11] A. Szabo, J. Lumin. 56 (1993) 47.
[12] (a) J. Ganem, Y.P. Wang, D. Boye, R.S. Meltzer, W.M. Yen, R.M. Macfarlane Phys. Rev. Lett. 66 (1991) 695.
(b) J. Ganem, Y.P. Wang, D. Boye, R.S. Meltzer, W.M. Yen, R. Wannemacher, R.M. Macfarlane, Phys. Rev. Lett. 66 (1991) 1649.
[13] D.E. McCumber, M.D. Sturge, J. Appl. Phys. 34 (1963) 1682.
[14] H. Riesen, B. Hayward, A. Szabo, A., J. Lumin. 127 (2007) 655.
[15] M. Blume, R. Orbach, A. Kiel, S. Geschwind, Phys. Rev. 139 (1965) A314.
[16] M. A. Kurnit, I. D. Abella, and S. R. Hartmann, in *The Physics of Quantum Electronics Conference Proceedings, San Juan, Puerto Rico, 1965*, edited by P. L. Kelley, B. Lax, and P. E. Tannenwald (McGraw-Hill, New York, 1966), p. 267.
[17] J. E. Rives, R. S. Meltzer, J.E. Rives, R.S. Meltzer, Phys. Rev. B 16 (1977) 1808.
[18] D. Hsu, J.L. Skinner, J. Chem. Phys. 83 (1985) 2107.
[19] J.T. Furukawa, T.B. Douglas, R.E. McCoskey, D.C. Ginnings, J. Res. Natl. Bur. Stand. 57(1956) 67.
[20] a) H. Riesen, L. Wallace, E. Krausz, Inorg. Chem. 39 (2000) 5044.
b) H. Riesen, E. Krausz, Chem. Phys. Lett. 287 (1998) 388.
[21] R.M. Macfarlane, J. Lumin. 85 (2000) 181.

Figure Captions

Figure 1 a) Polarized (solid line: σ-polarized; dashed line: π-polarized) absorption spectra, A(ν), of the R_2 transition of 20-ppm ruby (5 mm crystal) at 692 nm b) $R_2(\pm 1/2)$ transition of 0.6 ppm ruby (9 mm crystal) in σ polarization with (solid line) and without (dashed line) hole-burning; c) Unpolarized R_2 absorption spectra of a 20-ppm ruby (5 mm crystal) with (solid line) and without (dashed line) $R_2(\pm 1/2)$ hole-burning. The arrows indicate the resonant hole and the sidehole at +11.3 GHz of the resonant ions. The insert shows the region of the resonant hole; d) Unpolarized hole-burning difference spectrum, ΔA(ν), for a 130-ppm ruby sample. Arrows indicate the resonant and sidehole of the resonant ions. Hole-burning in b-d was conducted under pseudo-CW conditions (repetitive 1 ms burn period followed by a 400 μs readout period).

Figure 2 Temperature dependence (dashed line: 2.5 K; dash-dot line: 5 K; solid line 10 K) of σ-polarized hole-burning spectra, ΔA(ν), in the $R_2(\pm 1/2)$ line of 130 ppm ruby under a) pseudo-CW excitation (repetitive 1 ms burn period followed by a 400 μs readout period) and for b) pulsed experiments (1 Hz pulse repetition rate; 3.5 ms burn pulse; 400 μs readout period). In the pseudo-CW experiments of a) the background absorbance is severely diminished and the plot in Fig 2a shows ΔA *relative* to the background depletion (ΔA at low energy side of resonant hole offset to zero).

Figure 3 Pulsed σ-polarized transient hole-burning in the $R_2(\pm 1/2)$ line of 130 ppm ruby at 2.4 K with burn periods of 1.3, 2.6, 3.8, 5 and 6.2 ms (1 Hz repetition rate; 400 μs readout period).

Figure 4 a) Pulsed σ-polarized transient hole-burning, ΔA(ν), in the $R_2(\pm 1/2)$ line of 20 ppm ruby at 2.4 K with burn periods of 1.1, 2.6, 3.7, 5 and 6.2 ms (1 Hz repetition rate; 400 μs readout period). Panel b) shows the homogeneous linewidth ($\Gamma_h=1/2\Gamma_{hole}-\Gamma_{instr}$; $\Gamma_{instr}=2\times$laser linewidth=40 MHz) as a function of the relative holedepth ΔA/A.

Figure 5 Temperature dependence of the homogeneous linewidth, Γ_{hom}, of the R_2 line in ruby. The triangles and crosses display the results for the 130 and 20 ppm ruby samples, respectively, obtained by the transient hole-burning experiments of the present work. The squares show data from Figure 2 of reference 13 corrected for the low temperature residual (inhomogeneous) width. The solid line is calculated by using equation 2 with the parameters W=-0.277, T_D=935 K and Γ_0=142 MHz. The dashed and dash-dot lines show the contributions by the direct and Raman processes, respectively.

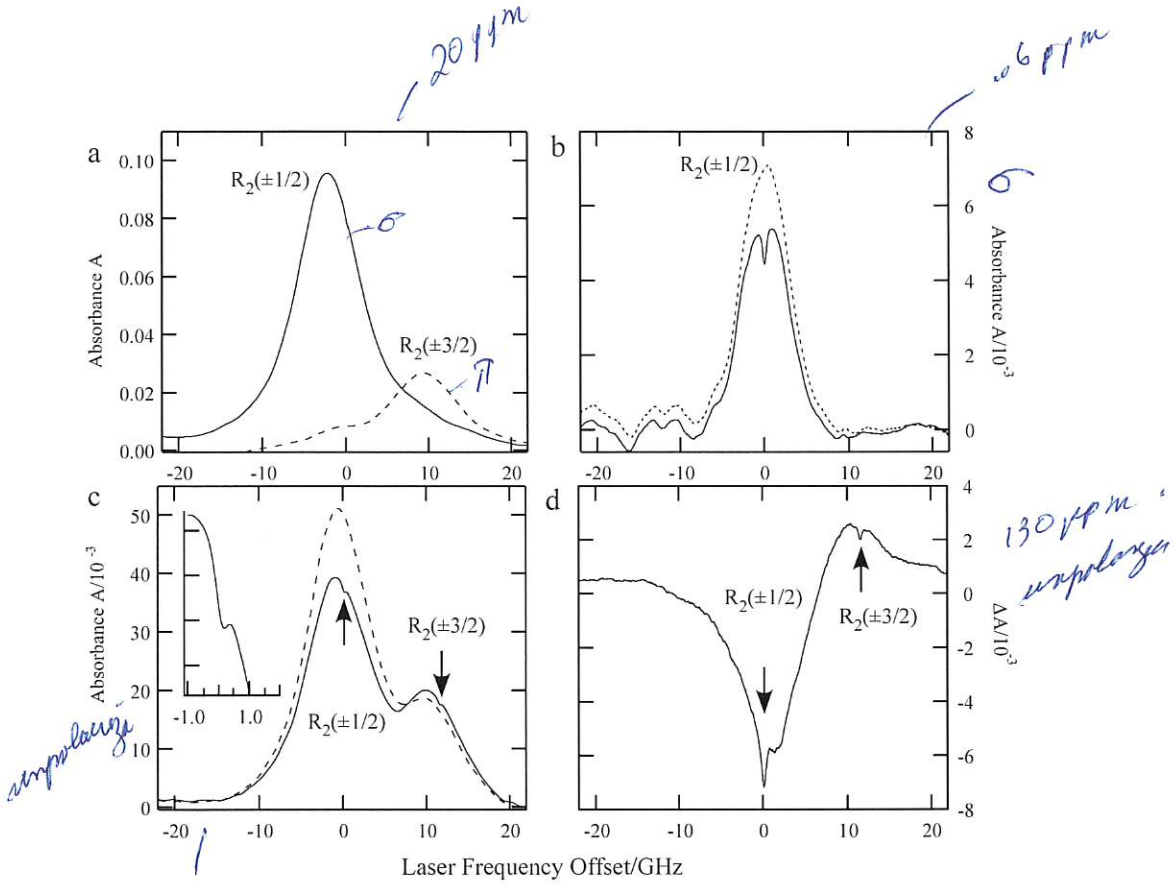
a
b
c
d
$R_2(\pm1/2)$
$R_2(\pm3/2)$
Absorbance A
Absorbance A/10^{-3}
ΔA/10^{-3}
Laser Frequency Offset/GHz

Figure 1

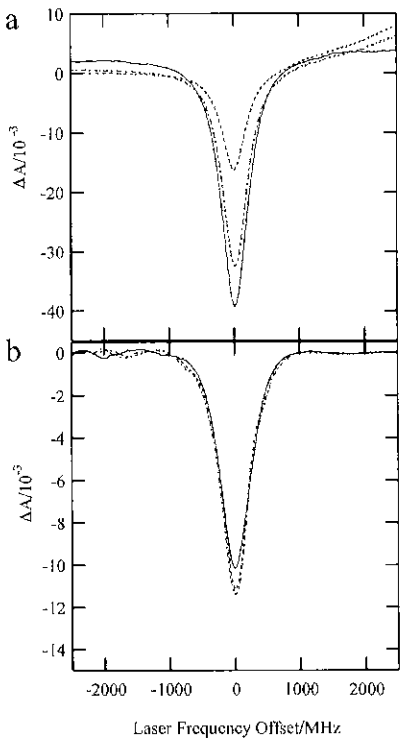

Figure 2

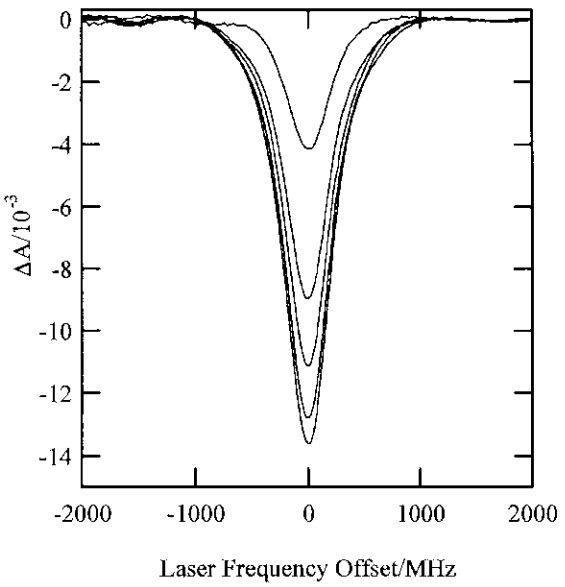
0
-2
-4
-6
-8
-10
-12
-14
ΔA/10^-3
-2000
-1000
0
1000
2000
Laser Frequency Offset/MHz

Figure 3

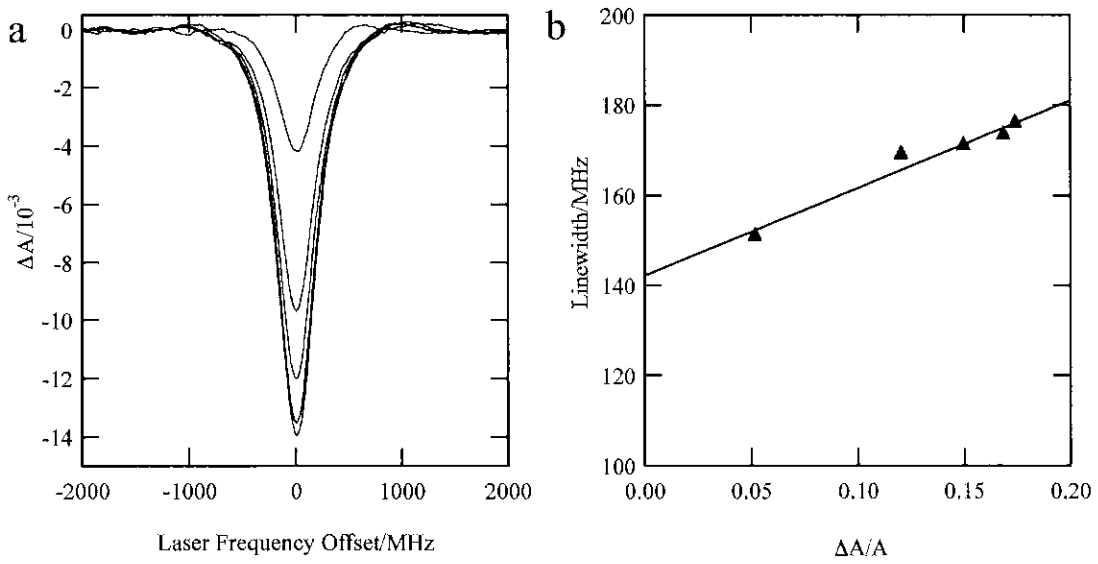
a
0
-2
-4
-6
-8
-10
-12
-14
ΔA/10^-3
-2000
-1000
0
1000
2000
Laser Frequency Offset/MHz
b
200
180
160
140
120
100
Linewidth/MHz
0.00
0.05
0.10
0.15
0.20
ΔA/A

Figure 4

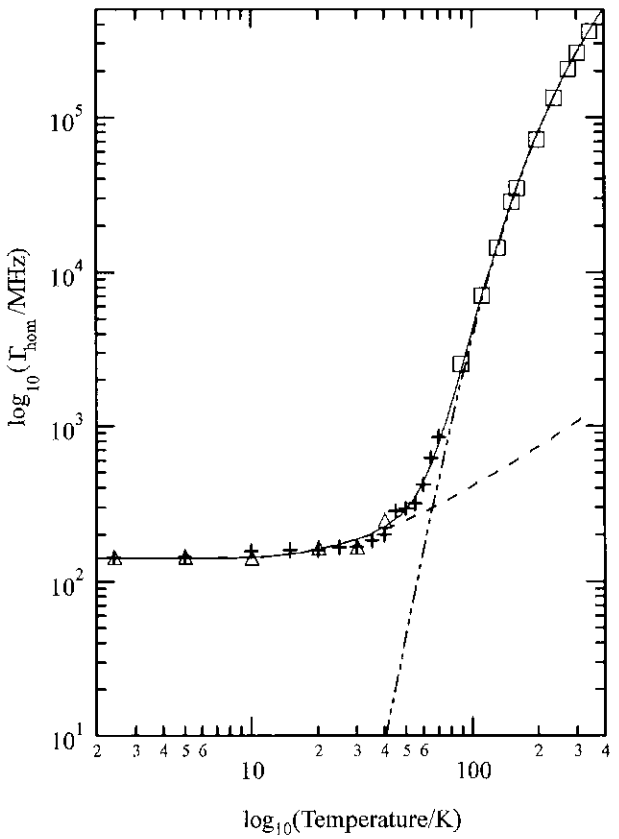
10^5
10^4
10^3
10^2
10^1
$\log_{10}(\Gamma_{hom}/MHz)$
2 3 4 5 6
10
2 3 4 5 6
100
2 3 4
$\log_{10}$(Temperature/K)

Figure 5